Quantum Electronics **30** (10) 932 – 936 (2000)

LASER APPLICATIONS AND OTHER TOPICS IN QUANTUM ELECTRONICS

PACS numbers: 42.62.Fi; 33.50.Dq
DOI: 10.1070/QE2000v030n10ABEH001836

On the uniqueness of the solution of inverse problems in saturation fluorimetry of polyatomic organic compounds

O V Kozyreva, K V Popov

Abstract. The theoretical and practical uniqueness of the results obtained by the method of nonlinear laser fluorimetry is considered. The theoretical uniqueness of measuring three basic photophysical parameters (the absorption cross section, the excited-state lifetime, and the quantum yield of intersystem crossing) from fluorescence saturation curves is proved rigorously mathematically. The practical uniqueness of the results obtained by this method is proved by the measurements of the absorption cross section and the excited-state lifetime from the calculated curves of fluorescence saturation simulating fluorescence saturation of aqueous solutions of rhodamine 6G, eosin, and Bengal rose dyes.

1. Introduction

One of the methods of laser spectroscopy used for diagnostics of organic compounds and complexes is the laser fluorimetry. The central problem of such diagnostics is the identification of the states of these complexes, which is required for measuring their concentration. To solve these problem, the method of laser saturation fluorimetry has been suggested [1, 2], which is based on the fact that the shape of fluorescence saturation curves of organic compounds depends on their photophysical parameters, such as the cross section for fluorescence excitation, the probability of intersystem crossing, the probability of singlet–singlet annihilation, the excited-state lifetime of molecules, etc. Analysis of fluorescence saturation curves allows one, in principle, to determine these parameters, i.e., to solve the inverse problem of the laser saturation fluorimetry.

Therefore, the inverse problem under study consists in the determination of the above parameters and (or) their combination from the measured fluorescence saturation curve, which represents the dependence of the number N_{fl} of detected photons on the flux density F of photons of exciting radiation (Fig. 1). This concerns not only organic dyes (and related compounds) but also large natural organic complexes such as cells of photosynthesising organisms, humus, protein compounds, complexes of hydrocarbons in petroleum, etc.

O V Kozyreva Department of Physics, M V Lomonosov Moscow State University, Vorob'evy Gory, 119899 Moscow, Russia
K V Popov Research Computing Center, M V Lomonosov Moscow State University, Vorob'evy Gory, 119899 Moscow, Russia

Received 19 July 1999
Kvantovaya Elektronika **30** (10) 932 – 936 (2000)
Translated by M N Sapozhnikov

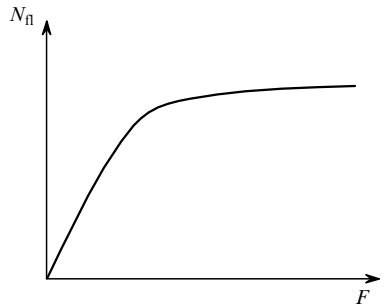

Figure 1. Typical dye fluorescence saturation curve.

2. Statement of the inverse problem of saturation fluorimetry

We studied low-concentration aqueous solutions of dyes ($C < 10^{-5}$ mol l^{-1}). The intermolecular interaction between dye molecules can be neglected at such low concentrations, and we can use in our physical model only parameters related to intramolecular processes. In this case, photophysical processes proceeding in dye solutions upon laser excitation can be described using a simple three-level model (Fig. 2), which includes the following processes: absorption of light, radiative and nonradiative relaxation of the first excited singlet state S_1, and intersystem crossing. Transitions from the T_1 triplet state to the ground S_0 state are ignored because the duration of the exciting laser pulse ($\sim 10^{-8}$ s) is substantially shorter than the triplet-state lifetime. The corresponding mathematical model represents a system of kinetic equations with three parameters: absorption cross section σ_{13}, the excited-state lifetime $t_3 = K_3^{-1}$, and the triplet-state quantum yield $\eta_T = K_{32}/K_3$:

$$\frac{\partial n_1(t,\boldsymbol{r})}{\partial t} = \left(K_{31} + K'_{31}\right) n_3(t,\boldsymbol{r}) - F(t,\boldsymbol{r})\sigma_{13} n_1(t,\boldsymbol{r}),$$

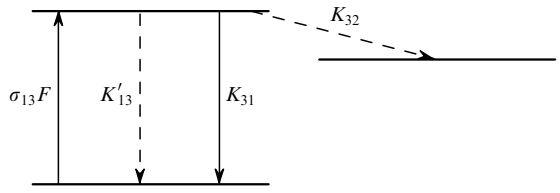

Figure 2. Three-level energy diagram for polyatomic organic molecules neglecting intermolecular interactions.

$$\frac{\partial n_2(t,\boldsymbol{r})}{\partial t} = K_{32} n_3(t,\boldsymbol{r}),$$

$$\frac{\partial n_3(t,\boldsymbol{r})}{\partial t} = F(t,\boldsymbol{r})\sigma_{13} n_1(t,\boldsymbol{r}) - K_3 n_3(t,\boldsymbol{r}), \tag{1}$$

$$n_1 + n_2 + n_3 = n_0,$$

where $F(t,\boldsymbol{r})$ is the flux density of exciting photons as a function of time t and coordinate $\boldsymbol{r} = \{x, y\}$ in the beam cross section; n_1, n_2, and n_3 are the populations of levels S_0, T_1, and S_1, respectively; $K_3 = K_{31} + K'_{31} + K_{32}$; K_{31} and K'_{31} are the rates of radiative and nonradiative $S_1 \to S_0$ transitions; and K_{32} is the rate of the $S_1 \to T_1$ transition. Because the dye solution layer of thickness l is assumed optically thin ($\sigma_{13} n_0 l \ll 1$), the dependence on the coordinate z along the beam is absent. The calculations were performed for the distribution of the photon flux density F that was rectangular over $\boldsymbol{r}$ and t.

The number N_{fl} of fluorescence photons emitted by the solution volume $V = Sl$ (where S is the beam cross section area and l is the layer thickness) excited by a laser pulse is

$$N_{\text{fl}} = K_{31} l \int_0^\infty \mathrm{d}t \int_S \mathrm{d}\boldsymbol{r} n_3(t,\boldsymbol{r}). \tag{2}$$

3. Analysis of stability and uniqueness of the inverse problem solution

The most important aspect of the inverse problem solution is the study of its uniqueness and stability with respect to errors in the input data (correctness of the problem statement). The theoretical stability of the inverse problem solution is ensured by the fact that the number of the required parameters is finite and the region of their variation is restricted [3].

We studied the uniqueness of the solution for a specified distribution of the photon flux density in space and time in the following way. Let us represent the system of equations (1) in the form

$$\frac{\mathrm{d}n_3}{\mathrm{d}t} = \sigma F n_1 - a_1 n_3,$$

$$\frac{\mathrm{d}n_1}{\mathrm{d}t} = -\sigma F n_1 + a_2 n_3, \tag{3}$$

where $n_3(0) = 0$; $n_1(0) = n_0$; $F(t) \equiv F$ for $0 \leqslant t \leqslant \tau_{\text{p}}$; $F(t) \equiv 0$ for $t \geqslant \tau_{\text{p}}$; τ_{p} is the laser pulse length; $a_1 = K_3$; $a_2 = K_{31} + K'_{31}$; and $\sigma = \sigma_{13}$. By solving the system of Eqns (3), we obtain

$$n_3(t) = C_0 \exp(-m_1 t) - C_0 \exp(-m_2 t)$$

$$+ C_0[\exp(-m_2\tau_{\text{p}}) - \exp(-m_1\tau_{\text{p}})]\exp(a_1\tau_{\text{p}})\exp(-a_1 t), \tag{4}$$

where

$$m_{1,2} = -k_{1,2} = \frac{1}{2}\left\{\sigma F + a_1 \mp \left[(\sigma F - a_1)^2 + 4\sigma F a_2\right]^{1/2}\right\}. \tag{5}$$

By integrating (4), we obtain the expression for $N_{\text{fl}}(F)$:

$$N_{\text{fl}} = K_{31}\int_0^{\tau_{\text{p}}} n_3(t)\mathrm{d}t = \frac{K_{31}C_0}{m_1}\left[1 - \exp(-m_1\tau_{\text{p}})\right]$$

$$- \frac{K_{31}C_0}{m_2}\left[1 - \exp(-m_2\tau_{\text{p}})\right]$$

$$+ \frac{K_{31}C_0}{a_1}\left[\exp(-m_1\tau_{\text{p}}) - \exp(-m_2\tau_{\text{p}})\right], \tag{6}$$

where

$$C_0 = \frac{\sigma F n_0}{\left[(\sigma F - a_1)^2 + 4\sigma F a_2\right]^{1/2}}.$$

The function $N_{\text{fl}}(F)$ defined in such an interval $[F_1, F_2]$, that $0 \leqslant F_1 \leqslant F_2$, is unique in the vicinity of points $F = 0$ and $F = \pm\infty$.

To prove the uniqueness of the solution, we took asymptotics of the function $N_{\text{fl}}(F)$ for $F \to \pm\infty$ and also the asymptotics of the limit

$$\lim_{F\to 0}\frac{\mathrm{d}N_{\text{fl}}(F)}{\mathrm{d}F}.$$

Let us show that the asymptotics of $N_{\text{fl}}(F)$ for $F \to -\infty$ determines uniquely the parameter σ. It follows from expression (6) that

$$\lim_{F\to-\infty} N_{\text{fl}} = \lim_{F\to-\infty}[\beta_1(F)\exp(\sigma|F|) + \beta_2(F)], \tag{7}$$

where functions β_1 and β_2 have finite limits for $F \to -\infty$ and

$$\lim_{F\to-\infty}\beta_1(F) = -\frac{K_{31}n_0}{a_1}\exp\tau_{\text{p}} \neq 0. \tag{8}$$

Let us prove that the rate of growth of the exponential at infinity determines uniquely the parameter σ. To do this, we assume that two different parameters – σ_1 and σ_2 correspond to the same N_{fl} for $F \to \infty$. In this case, we obtain from expression (7)

$$\lim_{F\to-\infty}\left(N_{\text{fl}}^{(\sigma_1)} - N_{\text{fl}}^{(\sigma_2)}\right) = \lim_{F\to-\infty}\Big[\beta_2^{(\sigma_1)} - \beta_2^{(\sigma_2)}$$

$$+ \beta_1^{(\sigma_1)}\exp(\sigma_1|F|) - \beta_1^{(\sigma_2)}\exp(\sigma_2|F|)\Big] \equiv 0. \tag{9}$$

Let us assume that $\sigma_2 < \sigma_1$. In this case, we have

$$\lim_{F\to-\infty}\left[N_{\text{fl}}^{(\sigma_1)} - N_{\text{fl}}^{(\sigma_2)}\right] = \lim_{F\to-\infty}\underset{\Downarrow\ \infty}{\exp\,(\sigma_1|F|)}$$

$$\times\left\{\beta_2^{(\sigma_1)}\underset{\Downarrow\ 0}{\exp\,(-\sigma_1|F|)} - \beta_2^{(\sigma_2)}\underset{\Downarrow\ 0}{\exp\,(-\sigma_1|F|)}\right. \tag{10}$$

$$\left.+\ \underset{\Downarrow\ \text{const}\neq 0}{\beta_1^{(\sigma_1)}} - \underset{\Downarrow\ 0}{\beta_1^{(\sigma_2)}}\underset{\Downarrow\ 0}{\exp[-(\sigma_1-\sigma_2)|F|]}\right\} = \infty.$$

Thus, the parameter σ is uniquely determined by the rate of growth of the exponential. Then, knowing σ, from

$$\left.\frac{\mathrm{d}N_{\text{fl}}}{\mathrm{d}F}\right|_{F=0} = K_{31}\frac{\sigma n_0\tau_{\text{p}}}{a_1} \tag{11}$$

we determine $a_1 = 1/t_3$.

To find $K_{32} = a_1 - a_2$, consider the asymptotics $N_{\text{fl}}(\infty)$:

$$\lim_{F\to\infty} N_{\text{fl}} = N_{\text{fl}}^{\infty} = \frac{K_{31}n_0}{a_1 - a_2}\left\{1 - \exp\left[-(a_1 - a_2)\tau_{\text{p}}\right]\right\} + \frac{K_{31}C_0}{a_1}\exp\left[-(a_1 - a_2)\tau_{\text{p}}\right]. \quad (12)$$

Let us show that the function $a_1 = f(a_1 - a_2)$ defined by expression (12) is monotonic. It follows from (12) that

$$a_1 = \frac{K_{31}n_0}{N_{\text{fl}}^{\infty}\exp x + K_{31}n_0\tau_{\text{p}}x^{-1}(1 - \exp x)}, \quad (13)$$

where $x = (a_1 - a_2)\tau_{\text{p}}$. It follows from (13) that

$$a_1'(x) = -\frac{K_{31}n_0\left[N_{\text{fl}}^{\infty}\exp x + K_{31}n_0\tau_{\text{p}}x^{-2}(\exp x - 1)\right]}{\left[N_{\text{fl}}^{\infty}\exp x + K_{31}n_0\tau_{\text{p}}x^{-1}(1 - \exp x)\right]^2} < 0. \quad (14)$$

Thus, the function $a_1(x)$ monotonically decreases everywhere in the region $x \in [0,\infty)$, and the dependence $\tau_{\text{p}}(a_1 - a_2) = \tau_{\text{p}}K_{32} = \varphi(a_1)$ is unique. Therefore, knowing a_1, one can uniquely determine $a_1 - a_2 \equiv K_{32}$.

Thus, parameters σ_{13}, t_3, and η_T can be uniquely determined from the fluorescence saturation curve within the framework of the fluorescence model chosen. A more complicated model, which considers non-rectangular distributions of F over the cross section and in time, takes into account intermolecular interactions, etc., would require an additional proof of the uniqueness. However, the analysis of the saturation curve shows its monotonic dependence on all real photophysical parameters, which allows one to expect that the uniqueness is also retained in more complicated cases.

4. Solution of the inverse problem of saturation fluorimetry

We solved the inverse problem by minimising the function that estimates the root-mean-square deviation of the data calculated within the framework of a physical model from the experimental data. We found that this function of many variables has several local minima and a complex 'gully' structure, which strongly hinders the minimisation process. For this reason, the minimisation was performed by the quasi-Newton method, which uses a gradient calculated analytically and a specific nature of the function being calculated, namely, the fact that it is determined by a sum of squares [4]. The method consists in the following: At each algorithm step, instead of the residual function, the function

$$f(\boldsymbol{X} + \Delta\boldsymbol{X}) = f(\boldsymbol{X}) + 2(J^{\text{t}}\varphi, \Delta\boldsymbol{X}) + (H\Delta\boldsymbol{X}, \Delta\boldsymbol{X}), \quad (15)$$

which approximates the residual function is minimised. Here, $\boldsymbol{X}$ is the vector of parameters; $\Delta\boldsymbol{X}$ is the vector of their increments; φ is the solution of the direct problem (in our case, this is an analytic solution for $N_{\text{fl}}(F)$ for the rectangular distribution of F in time and space); J^{t} is the transposed Jacobi matrix for the direct problem; and H is the symmetric quadratic matrix with elements

$$H_{ij} = \left(J^{\text{t}}J\right)_{ij} + \sum_k \frac{\varphi_k \partial^2\varphi_k}{\partial x_i \partial x_j}, \quad (16)$$

where φ_k is the solution of the direct problem at the kth point: and x_i and x_j are the ith and jth parameters (in our case, σ_{13} and t_3).

The possibilities of the variation approach were tested for low-concentration aqueous solutions of three dyes with different values of photophysical parameters. The above algorithm was used for solving the two-parametric inverse problem (we determined the absorption cross section σ_{13} and the excited-state lifetime t_3 in the case of a rectangular distribution of the laser pulse in time and space) with the help of model fluorescence saturation curves of aqueous solutions of rhodamine 6G, eosin, and Bengal rose dyes. The initial values of photophysical parameters used in Tables 1 – 4 were taken from paper [5]. The model saturation curves were made 'noisy' in calculations (the added noise was from 1 to 10 %).

Table 1 presents the results obtained. One can see that the errors of the reconstructed parameters proved to be even smaller than the errors of the initial data. This result, which appears unexpected at first glance, is explained by the fact that we managed to obtain an analytic expression for the saturation curve in a simplest case under study and thereby to eliminate the errors that would appear in the numerical solution of the system (1). In a certain sense, the results presented in Table 1 reflect the limiting possibilities of the method.

Then, we used this method to find two parameters (the third parameter being specified) in the case of a 'rectangular' distribution of the laser pulse in space and time. We reconstructed parameters σ_{13} and t_3 (the parameter η_T being specified), t_3 and η_T (the parameter σ_{13} being specified), and σ_{13} and η_T (the parameter t_3 being specified).

The values of parameters determined in the numerical experiment for the same dyes are presented in Tables 2 – 4. The parameters of rhodamine 6G and eosin were reconstructed with good accuracy. However, in the determination of parameters of Bengal rose the practical instability was manifested as local minima with parameters t_3 that strongly differed from real ones, although lied in the region of the solution search. This is obviously explained by the fact that the triplet quantum yield for Bengal rose is very high (close to unity), whereas the value of t_3 is very small. Nevertheless, we managed to overcome the practical instability in the reconstruction of parameters σ_{13} and t_3, with η_T being specified, and in the reconstruction of parameters t_3 and η_T, with σ_{13} being specified, by using *a priori* information obtained in the study of the direct problem: the absolute values of N_{fl} on a plateau strongly differ for different t_3, so that the order of magnitude of t_3 can be readily estimated.

However, the practical instability remained (as one can see from Table 3) in the problem of determining η_T and σ_{13} (with t_3 being specified). This question is a subject of further studies.

Our preliminary calculations showed that complication of the problem (consideration of non-rectangular distributions of F, calculation of three parameters instead of two) drastically increases the dispersion, especially for the three-parametric problem, and makes the dispersion substantially greater than the noise of the initial data (resulting sometimes in the practical instability [4]).

We continue to study algorithms for solving such more complicated problems. In this paper, we restricted ourselves

Table 1. Parameters σ_{13} and t_3 obtained from model curves by the variation method.

Dye	Noise (%)	$\langle\sigma_{13}\rangle/10^{-16}$ cm^2	Dispersion (%)	$\langle t_3\rangle$/ns	Dispersion (%)
Rhodamine 6G	Real	2.50	–	4.00	–
	0	2.50	–	4.00	–
	1	2.50	0.1	4.00	0.1
	3	2.50	0.5	3.98	0.5
	5	2.50	0.7	3.97	0.7
	10	2.54	1.2	4.03	1.0
Eosin	Real	1.10	–	1.40	–
	0	1.10	–	1.40	–
	1	1.10	0.1	1.40	0.3
	3	1.10	0.3	1.39	1.0
	5	1.10	0.4	1.41	1.4
	10	1.10	1.0	1.37	3.5
Bengal rose	Real	1.20	–	0.10	–
	0	1.20	–	0.10	–
	1	1.20	0.1	0.10	2.0
	3	1.21	0.2	0.11	5.0
	5	1.21	0.3	0.12	7.0
	10	1.22	0.5	0.14	8.0

Table 2. Parameters σ_{13} and t_3 of three dyes obtained, with η_T being specified, by the method of least squares.

Dye	Noise (%)	$\langle\sigma_{13}\rangle/10^{-16}$ см^2	Dispersion (%)	$\langle t_3\rangle$/ns	Dispersion (%)
Rhodamine 6G	Real	2.50	–	4.00	–
	0	2.50	–	4.00	–
	1	2.50	0.01	3.93	0.1
	3	2.50	0.01	3.92	0.3
	5	2.50	0.01	3.92	0.7
	10	2.50	0.2	3.94	0.8
Eosin	Real	1.10	–	1.40	–
	0	1.09	–	1.40	–
	1	1.10	0.2	1.41	1.5
	3	1.10	1.0	1.33	7.4
	5	1.10	1.3	1.27	11.0
	10	1.09	2.6	1.21	18.8
Bengal rose	Real	1.20	–	0.10	–
	0	1.20	–	0.10	–
	1	1.20	0.1	0.10	0.01
	3	1.22	0.5	0.10	0.01
	5	1.19	0.7	0.10	0.01
	10	1.17	1.0	0.10	0.01

Table 3. Parameters σ_{13} and η_T of three dyes obtained, with t_3 being specified, by the method of least squares.

Dye	Noise (%)	$\langle\sigma_{13}\rangle/10^{-16}$ cm^2	Dispersion (%)	$\langle\eta_T\rangle$	Dispersion (%)
Rhodamine 6G	Real	2.50	–	0.002	–
	0	2.50	–	0.002	–
	1	2.50	0.2	0.002	0.1
	3	2.54	1.1	0.002	0.2
	5	2.59	1.9	0.002	0.3
	10	2.59	1.9	0.002	0.6
Eosin	Real	1.10	–	0.68	–
	0	1.10	–	0.68	–
	1	1.10	0.6	0.68	0.4
	3	1.06	2.5	0.70	2.1
	5	0.97	5.6	0.78	4.8
	10	1.02	11.5	0.78	7.7
Bengal rose	Real	1.20	–	0.95	–
	0	1.70	–	0.66	–
	1	1.70	10.3	0.74	10.1
	3	1.65	13.3	0.79	11.3
	5	1.96	9.8	0.65	12.2
	10	2.15	8.7	0.57	12.5

Table 4. Parameters t_3 and η_T of three dyes obtained, with σ_{13} being specified, by the method of least squares.

Dye	Noise (%)	$\langle t_3 \rangle$/ns	Dispersion (%)	$\langle \eta_t \rangle$	Dispersion (%)
Rhodamine 6G	Real	4.00	–	0.002	–
	0	4.00	–	0.002	–
	1	4.03	0.3	0.002	0.2
	3	4.03	0.9	0.002	0.6
	5	3.93	1.9	0.002	1.0
	10	4.08	4.7	0.002	2.7
Eosin	Real	1.40	–	0.68	–
	0	1.40	–	0.68	–
	1	1.38	2.4	0.68	0.2
	3	1.14	10.2	0.67	0.7
	5	1.05	14.0	0.67	1.5
	10	1.05	32.4	0.69	2.2
Bengal rose	Real	0.10	–	0.95	–
	0	0.10	–	0.95	–
	1	0.10	0.01	0.96	0.2
	3	0.10	0.01	0.96	0.5
	5	0.10	0.01	0.96	1.1
	10	0.10	0.01	0.94	1.7

to the establishment of the possibility of solving inverse problems of nonlinear laser fluorimetry by considering the simplest case, as is usually done at the first stage.

Acknowledgements. This work was supported by the Russian Foundation for Basic Research (Grant No 99-02-17946), the 'Fundamental Spectroscopy' program of the Russian Federation State Committee on Science and Technology (Grant No 1.6), and the Federal Specific Program 'Integration' (Teaching and Research Centre 'Fundamental Optics and Spectroscopy').

References

1. Fadeev V V, Chekalyuk A M, Demidov A A, Abroskin A G, Malinina E L, Maslyukova L L, Shanta I *Trudy III Konferentsii po Lyuminestsentsii* (Proceedings of III Conference on Luminescence) (Seged: Hungary, 1979), p. 149
2. Fadeev V V, Chekalyuk A M, Chubarov V V *Dokl. Akad. Nauk SSSR* **262** 338 (1982)
3. Tikhonov A N, Arsenin V Ya *Metody Resheniya Nekorrektnykh Zadach* (Methods for Solving Ill-Posed Problems) (Moscow: Nauka, 1979)
4. Tikhonravov A V, Trubetskov M K In: *Komp'yutery v Laboratorii* (Computers in Laboratory) (Moscow: Moscow State University, 1992), p. 32
5. Korobov V E, Chibisov A K *Usp. Khim.* **52** 43 (1983)